



Optical properties of photoresists for femtosecond 3D printing: refractive index, extinction, luminescence-dose dependence, aging, heat treatment and comparison between 1-photon and 2-photon exposure

MICHAEL SCHMID,^{*} DOMINIK LUDESCHER, AND HARALD GIESSEN

4th Physics Institute and Research Center SCoPE, University of Stuttgart, Pfaffenwaldring 57, 70569 Stuttgart, Germany

**m.schmid@pi4.uni-stuttgart.de*

Abstract: Femtosecond 3D printing has emerged as an important technology for manufacturing nano- and microscopic optical devices and elements. Detailed knowledge of the dispersion in the visible and near-infrared spectral range is crucial for the design of these optical elements. Here we provide refractive index measurements for different UV-doses, aging times, heat treatment and 2-photon exposed structures for the photoresists IP-S, IP-Dip, IP-L, OrmoComp, IP-Visio, and PO4. We use a modified and automatized Pulfrich refractometer setup, utilizing critical angles of total internal reflection with an accuracy of $5 \cdot 10^{-4}$ in the visible and near-infrared spectral range. We compare Cauchy and Sellmeier fits to the dispersion curves. We also give Abbe numbers and Schott Catalog numbers of the almost entirely polymerized resists. Additionally, we provide quantitative extinction and luminescence measurements for all photoresists.

© 2019 Optical Society of America under the terms of the [OSA Open Access Publishing Agreement](#)

1. Introduction

Over the last years, a large variety of micro- and nanooptical elements and even multi-element microobjectives have been demonstrated using 3D direct laser writing [1-19]. In order to optimize the imaging performance of micro- and nanooptical elements the detailed knowledge of dispersion of the used photoresists is crucial. Furthermore, the knowledge of the dispersion of different optical materials enables the construction of optical devices with achromatic functionality, as recently demonstrated [1]. The degree of polymerization of different photoresists, and therefore their optical properties such as refractive index and extinction, depends strongly on different parameters such as UV dose, aging time, 1- photon or 2-photon polymerization, and post processing (e.g. heat treatment and further UV exposure) [20].

Here we provide detailed, quantitative, and systematic measurements of the refractive index dependency of UV dose, aging, heat treatment, and 1- or 2-photon dependence. We measure the critical angle of total internal reflection with a modified and automatized Pulfrich refractometer setup, as depicted in Fig. 1.

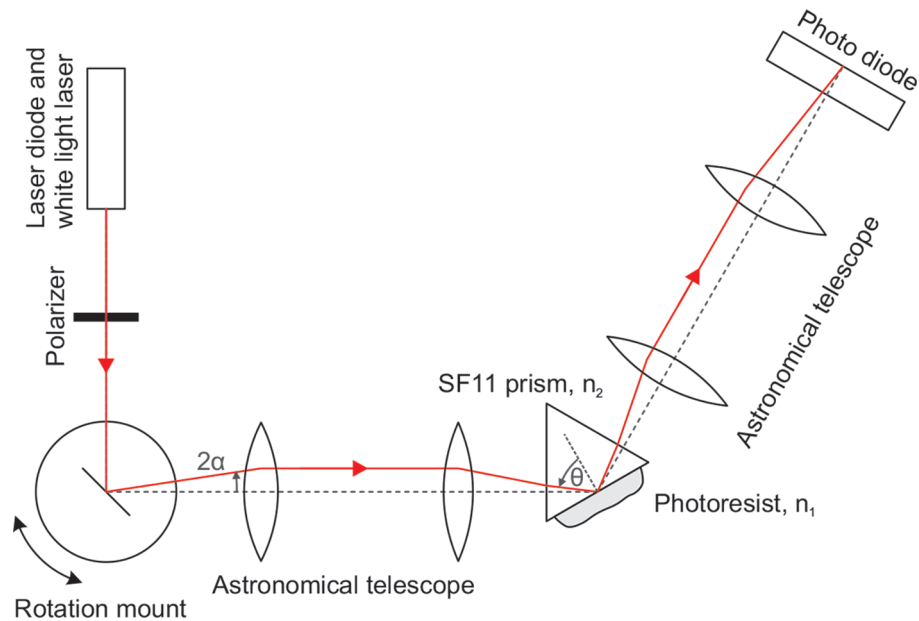


Fig. 1. Modified and automatized Pulfrich refractometer setup. The light source is a white light laser and an additional laser diode; the angle of incidence is controlled using a mirror on a rotation mount. Measurements are taken at room temperature.

2. Method

The linearly polarized light source is a tunable white light laser (NKT SuperK EXTREME) with an accessible range from 500 nm to 1400 nm. To further extend the accessible wavelength range we use an additional laser diode at 405 nm (Thorlabs CPS405 collimated laser diode module). The light is guided through an astronomical telescope onto the base of a N-SF11 prism where a reference material (N-BK7 plate) is optically bounded by pressure and the photoresist under investigation is hardened in an area right next to the reference plate. Using a mirror on a rotation mount the angle of the incident beam onto the base of the prism can be changed. The reflected light is guided through another astronomical telescope onto a photodiode which measures the angle-dependent intensity. The critical angle of total internal reflection is determined by measuring the reflected intensity depending on the angle of incidence on the base of the prism, which is controlled by the rotation mount. The angle of incidence can be calculated using basic trigonometric functions and Snell's law to

$$\begin{aligned} \theta(\alpha) &= 60^\circ + \arcsin \left[\frac{n}{n_2} \sin \left(\arctan \left(\frac{f_1}{f_2} \tan(2\alpha) \right) \right) \right] \\ &\approx 60^\circ + \frac{n}{n_2} \frac{f_1}{f_2} 2\alpha \text{ for small rotation angles } \alpha, \end{aligned} \quad (1)$$

with the rotation angle α of the rotation mount, n the refractive index of the surrounding medium (air) and n_2 the refractive index of the prism material. The astronomical telescope consists of two lenses with focal lengths of $f_1 = f_2 = 10$ cm. For the astronomical telescope the distance between the two lenses is equal to the sum of the two focal lengths $f_1 + f_2 = 20$ cm.

To calculate the refractive index of the photoresist we have to obtain the point of the critical angle of the prism/photoresist interface as well as for the prism/ BK7 glass interface to calibrate the incident angle.

Therefore, one part of the prism is coated with an approximately 2 mm thick layer of the photoresist and on the other part we optically bond a BK7 glass plate by pressure.

To obtain the critical angle we fit the corresponding reflectance given by Fresnel's equation

$$R_s = \left| \frac{n_1 \cos \theta - \sqrt{n_2^2 - n_1^2 \sin^2 \theta}}{n_1 \cos \theta + \sqrt{n_2^2 - n_1^2 \sin^2 \theta}} \right|^2 \quad (2)$$

for s-polarized light to the measured data. We achieve an accuracy of $5 \cdot 10^{-4}$, for additional information see [21].

3. Experimental details

The degree of polymerization of different photoresists and hence their refractive indices, depends strongly on different parameters such as UV dose, aging process, heat treatment, and 1-photon or 2-photon illumination [20,22]. In the following we present and discuss the typical refractive index behavior of the photoresists IP-S, IP-Dip, IP-L, and OrmoComop depending on these parameters.

3.1. UV dose dependency

To study the refractive index depending on the UV dose, we expose samples of each photoresist for different illumination times to a UV lamp (DymaxBlueWave 50 delivering 365 nm with an intensity of 3000 mW/cm², at a distance of 3 cm with resulting intensity of 250 mW/cm²) and measure the refractive index afterwards as described above. Figure 2 (a) illustrates the results for the different photoresists. As expected, the refractive index increases over the entire wavelength range with the UV exposure, however, with longer exposure times the refractive index change saturates and exhibits a limited growth behavior as depicted in Fig. 2 (b). This behavior can simply be explained with the polymerization process, which is triggered by UV light. As the exposure to UV light persists, the degree of polymerization increases but slows down as more and more areas of the photoresist become almost entirely polymerized. The same behavior has been observed in 2-photon polymerized samples of IP-Dip using different laser intensities [20].

This saturation behavior can be seen in all photoresists. However, it strongly depends on the UV sensitivity of each photoresist. The refractive index of IP-S and IP-L still rises after 30 minutes of UV duration, whereas IP-Dip is saturating. OrmoComp exhibits a much higher UV sensitivity and saturates within several seconds.

3.2. Aging process

The refractive index also depends on the aging process of the photoresists which is overall not as significant as the UV exposure. Post polymerization can take up to several days and further increases the refractive index after the initial UV exposure even without further UV treatment. After the photo initiators are activated by UV exposure the polymerization process starts. The activated photo initiator is slowly used up during the polymerization, which leads to a rise in the degree of polymerization and therefore the refractive index over time. To compare the effects of the aging process we expose the photoresists to the UV light for 15 minutes (250 mW/cm²) and measure the refractive indices directly after the exposure, after 24 hours, 48 hours, and 72 hours.

The refractive index slightly increases with the aging time as depicted in Fig. 3. However, the changes are below 10^{-3} except for IP-L, which has the strongest refractive index increase due to post polymerization, which occurs mainly within the first 24 hours. Measurements after a longer time period have also been taken but did not show a significant increase of the refractive indices.

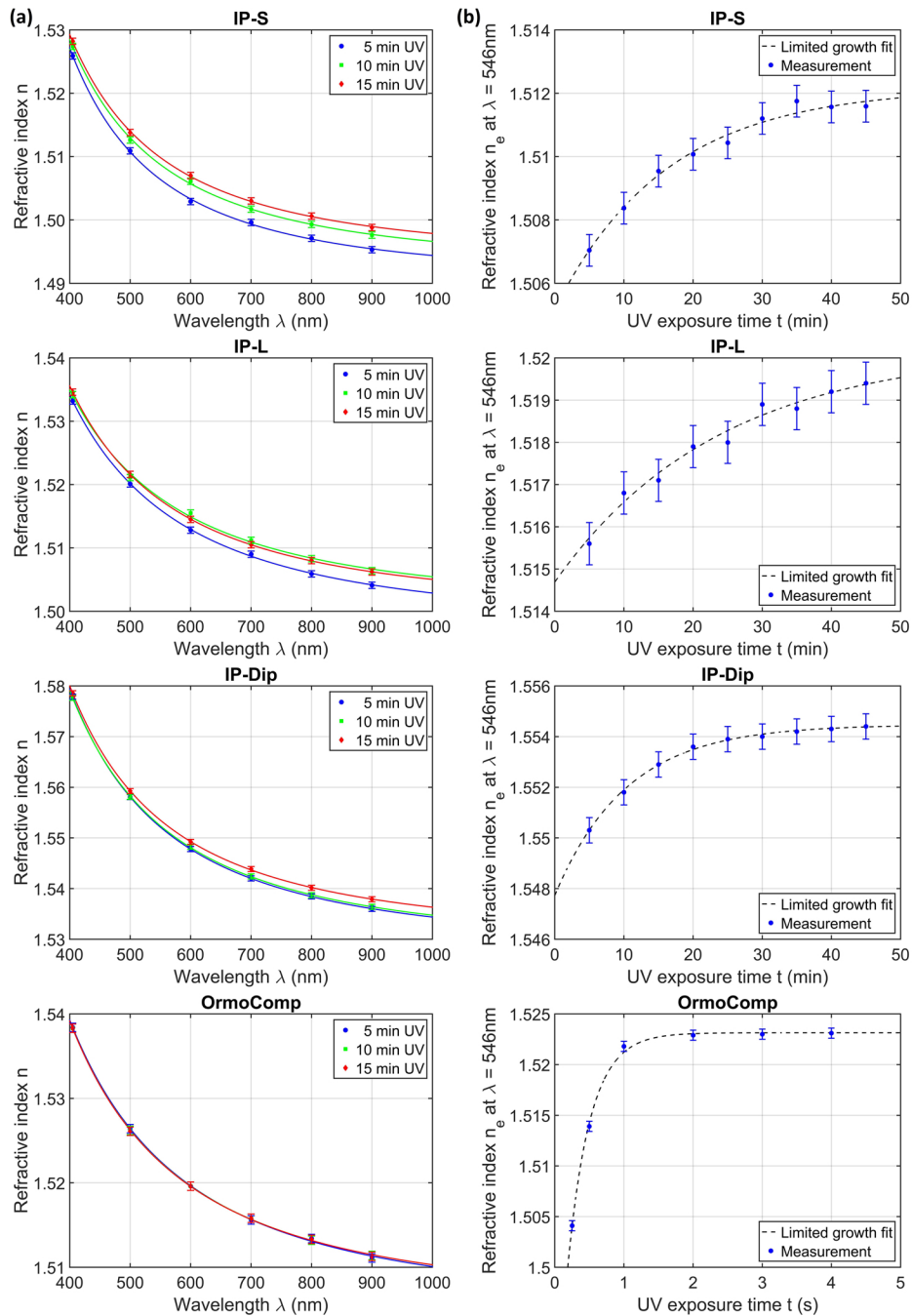


Fig. 2. Refractive index of the photoresists IP-S, IP-Dip, IP-L, and OrmoComp depending on the UV dose. For all photoresists the refractive index rises with longer UV curing times over the entire wavelength range (a). Closer investigation shows a saturation behavior of the refractive index depending on the UV dose (b). However, the saturation times vary; OrmoComp reaches saturation within several seconds, whereas the refractive indices of the other photoresists saturate after more than 30 minutes.

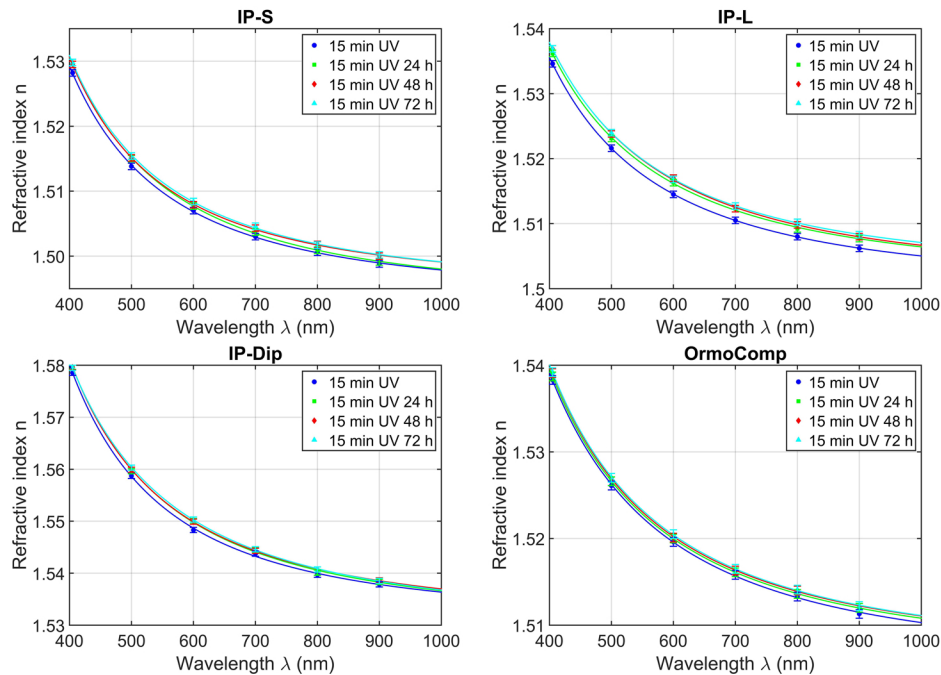


Fig. 3. Refractive index plotted for different aging times. Due to post polymerization the refractive index rises up to several days after the initial illumination. However, the change in the refractive index finally becomes very small.

3.3. Heat treatment

The refractive index of UV treated photoresists strongly depends on the photoresist itself, the UV curing time, and the aging process which leads to an uncertainty in predicting the finally obtained refractive indices. However, this problem can be solved using heat treatment (post baking) of the photoresists after the UV curing.

Different measurements have shown that 1-hour post baking at 60 °C is sufficient to reach a highly polymerized state for each of the investigated photoresists even with a low initial UV curing time of 5 minutes. Using heat treatment, we increase the reaction speed of the polymerization and therefore reach the saturation limit much faster. Furthermore, some photo initiators can be activated by higher temperatures. We also observed that the refractive indices did not change further over time because post polymerization cannot significantly influence the refractive index anymore. The refractive indices before and after the heat treatment are plotted in Fig. 4.

3.4. 2-photon polymerization

As recently shown for IP-Dip, the refractive index of photoresists after 2-photon polymerization also depends on the used laser intensity [20].

The 2-photon polymerized measurement patches are fabricated directly onto the back of the measurement prism using a 3D direct laser writer (Photonic Professional GT) with a 25x objective.

We perform 2-photon polymerized measurements for IP-S, IP-Dip, and OrmoComp. Due to sticking issues of the 2-photon polymerized photoresist with the prism it was not possible to perform the 2-photon polymerized measurement for IP-L with our method.

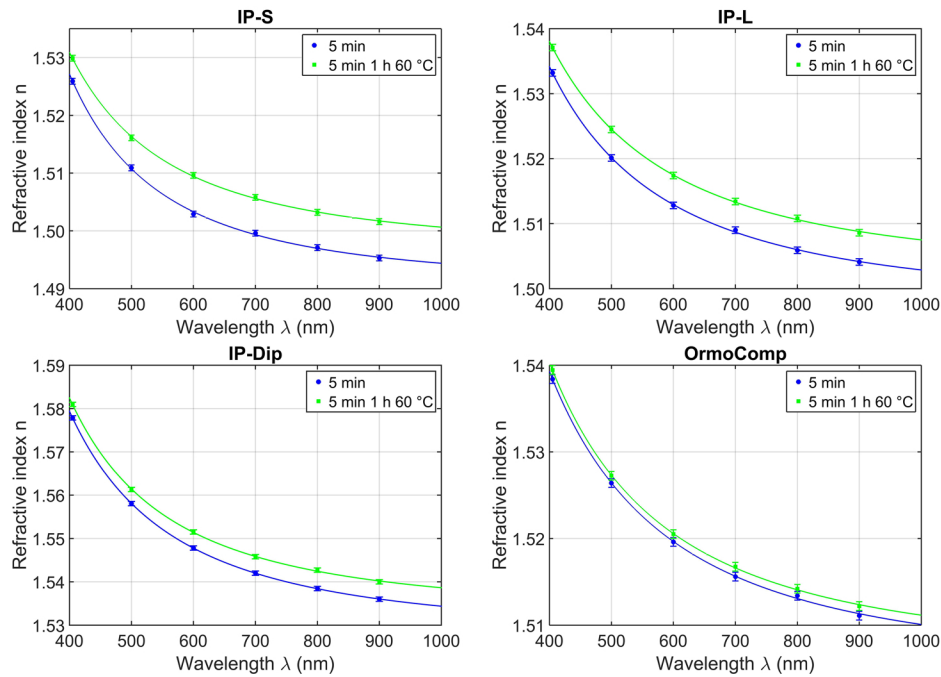


Fig. 4. Refractive indices after 5 minutes of UV curing before and after 1 hour heat treatment at 60 °C. The refractive indices of all photoresists significantly rise during the heat treatment and reach the same level as they have shown in Fig. 3 after 15 minutes UV treatment and additional post polymerization.

The results are similar to the almost entirely polymerized refractive indices after post baking of the UV cured samples except for IP-Dip (see Fig. 5). For this high-resolution photoresist the coarse slicing (2 μm) and hatching (0.8 μm) parameters required to write patches with sufficient size for the measurements in a reasonable time provided not enough intensity for complete polymerization. Therefore, the refractive index is almost as low as the refractive index of the liquid IP-Dip photoresist.

3.5. Heat treated wide spectral range measurements

Finally, we show the measured dispersion for the heat treated 1-photon polymerized photoresists IP-S, IP-L, IP-Dip, OrmoComp, IP-Visio, and PO4 after 15 minutes UV curing and 1-hour post baking at 60 °C between 405 nm and 1400 nm. The refractive indices did not further increase neither by additional UV exposure, nor aging. Therefore, we expect them to be almost completely polymerized.

As shown in Fig. 6 the Cauchy fit can describe the dispersion of the photoresists only up to a wavelength of about 900 nm-1000 nm. For higher wavelength a Sellmeier fit provides a much better match between our model and the measurements. The corresponding fit function are for the Cauchy fit

$$n(\lambda) = A + \frac{B}{\lambda^2} + \frac{C}{\lambda^4}, \quad (3)$$

and for the Sellmeier fit

$$n(\lambda)^2 = 1 + \frac{B_1 \lambda^2}{\lambda^2 - C_1} + \frac{B_2 \lambda^2}{\lambda^2 - C_2} + \frac{B_3 \lambda^2}{\lambda^2 - C_3}. \quad (4)$$

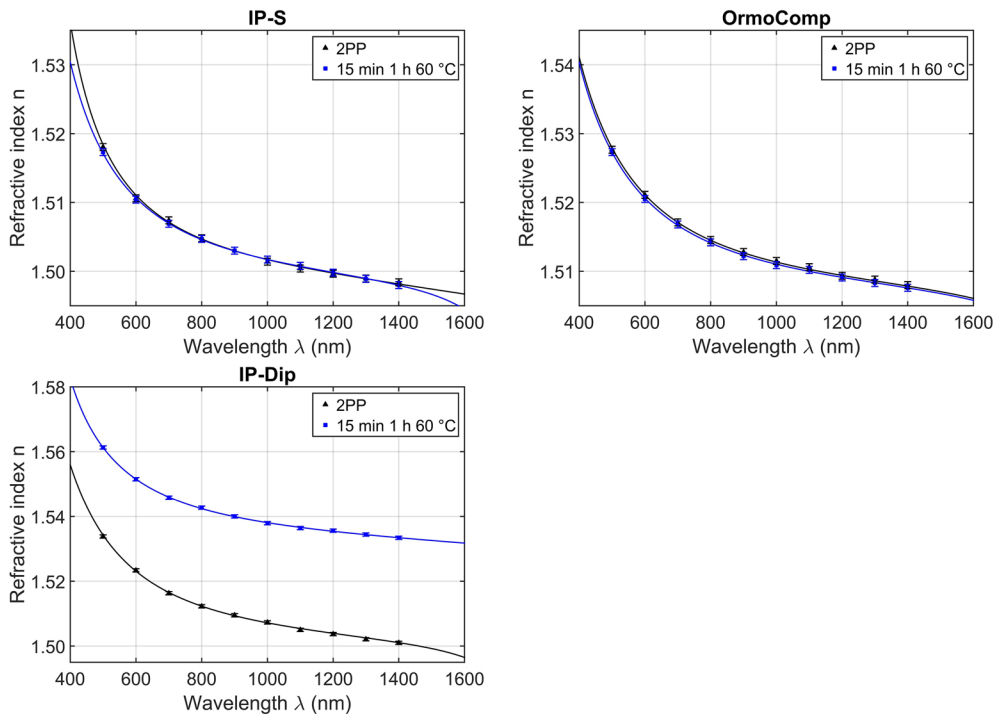


Fig. 5. The refractive index of 2-photon polymerized samples and 15 min UV 1 hour at 60 °C post baked samples in comparison with Sellmeier fits. The 2-photon polymerized samples of IP-S (Laser power: 70% Scan speed: 50000 $\mu\text{m}/\text{s}$ Slicing: 2 μm Hatching: 0.8 μm) and OrmoComp (Laser power: 100% Scan speed: 20000 $\mu\text{m}/\text{s}$ Slicing: 2 μm Hatching: 0.8 μm) show the same higher refractive index as the post baked samples except for the high-resolution resist IP-Dip (Laser power: 100% Scan speed: 40000 $\mu\text{m}/\text{s}$ Slicing: 2 μm Hatching: 0.8 μm). In this case the used slicing and hatching did not provide enough intensity to almost entirely cure the photoresist which results in a much lower refractive index.

The fit parameters are summarized in Table 1 and Table 2. The Sellmeier fit is performed using Zemax OpticStudio.

Table 1. Cauchy parameters for the photoresists IP-S, IP-Dip, IP-L, OrmoComp, IP-Visio, and PO4. We obtain the values by fitting the corresponding equation to the measured refractive index data.

Cauchy parameters	A	B	C
IP-S	1.4975	$4.2627 \cdot 10^{-3}$	$1.5925 \cdot 10^{-4}$
IP-Dip	1.5324	$5.8913 \cdot 10^{-3}$	$3.3848 \cdot 10^{-4}$
IP-L	1.5020	$5.4252 \cdot 10^{-3}$	$0.5437 \cdot 10^{-4}$
OrmoComp	1.5061	$4.9943 \cdot 10^{-3}$	$0.7781 \cdot 10^{-4}$
IP-Visio	1.4967	$4.8938 \cdot 10^{-3}$	$0.4882 \cdot 10^{-4}$
PO4	1.5928	$8.4142 \cdot 10^{-3}$	$7.4353 \cdot 10^{-4}$

Table 3 and Table 4 show the measured refractive indices, the corresponding Abbe number and Schott catalog number for each photoresist from 405 nm to 1400 nm after 15 minutes UV curing and post baking at 60 °C for 1 hour.

The refractive indices and dispersions can be visualized using an Abbe diagram as depicted in Fig. 7. Comparing the measurement results we find, that IP-S, IP-L, OrmoComp, and IP-Visio

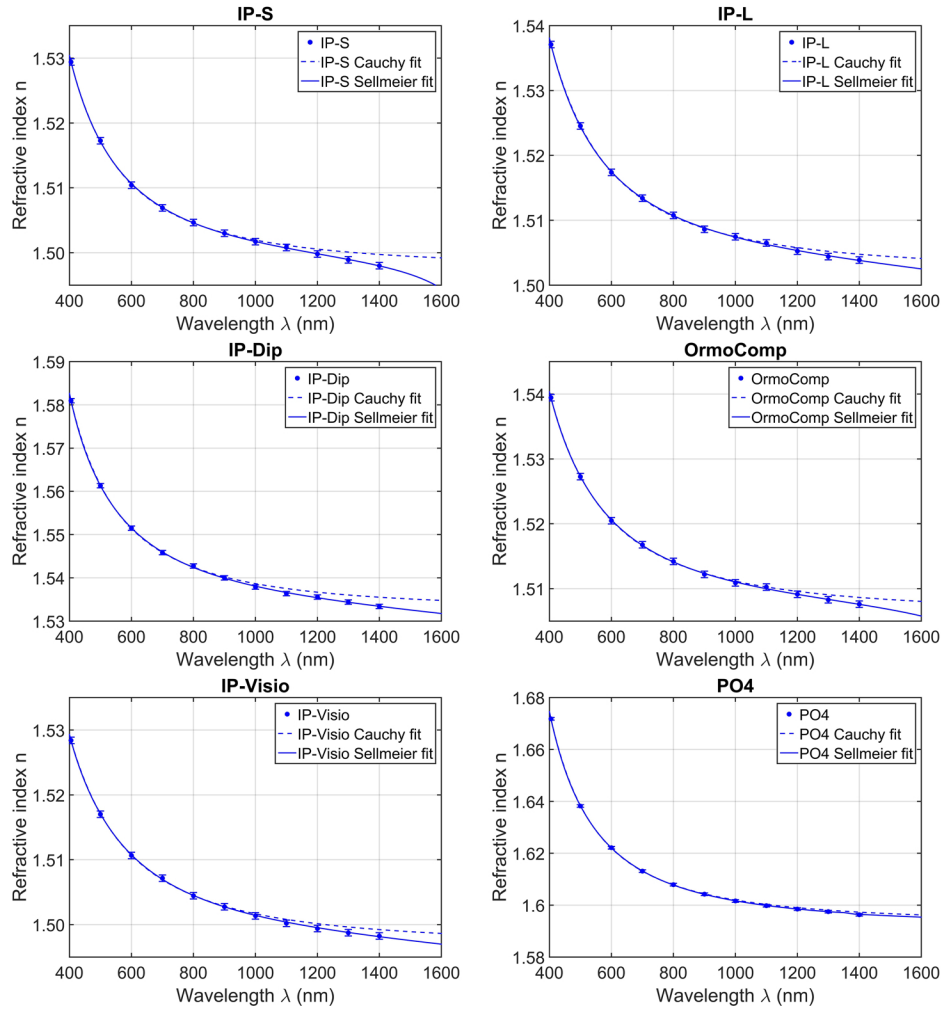


Fig. 6. Dispersion of the photoresists IP-S, IP-Dip, IP-L, OrmoComp, IP-Visio, and PO4 in the almost entirely polymerized state. The samples have been UV cured for 15 minutes and afterwards post baked at 60 °C for 1 hour. Further UV illumination, aging or heat treatment did only have minor effect on the refractive indices.

Table 2. Sellmeier parameters for the photoresists IP-S, IP-Dip, IP-L, OrmoComp, IP-Visio, and PO4. We obtain the values by fitting the corresponding equation to the measured refractive index data.

Sellmeier parameters	B_1	C_1 in μm^2	B_2	C_2 in μm^2	B_3	C_3 in μm^2
IP-S	$8.3794 \cdot 10^{-1}$	$1.4153 \cdot 10^{-6}$	$4.0620 \cdot 10^{-1}$	$3.1160 \cdot 10^{-2}$	$4.7704 \cdot 10^{-3}$	$3.3379 \cdot 10^0$
IP-Dip	$1.2899 \cdot 10^0$	$1.1283 \cdot 10^{-2}$	$6.0569 \cdot 10^{-2}$	$7.7762 \cdot 10^{-2}$	$1.1844 \cdot 10^5$	$2.5802 \cdot 10^7$
IP-L	$6.4426 \cdot 10^{-1}$	$1.5633 \cdot 10^{-3}$	$6.1654 \cdot 10^{-1}$	$2.2156 \cdot 10^{-2}$	$1.8721 \cdot 10^1$	$5.3055 \cdot 10^3$
OrmoComp	$1.2626 \cdot 10^0$	$1.1292 \cdot 10^{-2}$	$7.2386 \cdot 10^{-3}$	$7.9571 \cdot 10^{-2}$	$5.2295 \cdot 10^{-3}$	$4.1848 \cdot 10^0$
IP-Visio	$2.0815 \cdot 10^{-4}$	$1.4186 \cdot 10^{-1}$	$1.2427 \cdot 10^0$	$1.1332 \cdot 10^{-2}$	$5.3236 \cdot 10^4$	$1.8274 \cdot 10^7$
PO4	$1.0006 \cdot 10^0$	$3.8130 \cdot 10^{-3}$	$5.3251 \cdot 10^{-1}$	$5.0662 \cdot 10^{-2}$	$-2.289 \cdot 10^{-5}$	$1.9141 \cdot 10^0$

Table 3. Measured refractive indices of almost entirely polymerized photoresists (15 min UV, 1 hour at 60 °C post baking).

	405 nm	500 nm	600 nm	700 nm	800 nm	900 nm	1000 nm
IP-S	1.5294	1.5173	1.5104	1.5069	1.5047	1.5030	1.5017
IP-Dip	1.5810	1.5613	1.5515	1.5458	1.5427	1.5400	1.5379
IP-L	1.5371	1.5245	1.5174	1.5134	1.5108	1.5086	1.5075
OrmoComp	1.5394	1.5273	1.5205	1.5168	1.5142	1.5122	1.5109
IP-Visio	1.5284	1.5170	1.5107	1.5072	1.5045	1.5028	1.5014
PO4	1.6718	1.6382	1.6221	1.6131	1.6079	1.6042	1.6016

Table 4. Measured refractive indices of almost entirely polymerized photoresists (15 min UV, 1 hour at 60 °C post baking). The corresponding Abbe numbers and Schott catalog numbers are given in the last two columns.

1100 nm	1200 nm	1300 nm	1400 nm	Abbe number	Schott catalog number
1.5008	1.4998	1.4989	1.4980	50.45	511504
1.5364	1.5356	1.5344	1.5334	35.67	552357
1.5065	1.5052	1.5044	1.5039	46.93	518469
1.5102	1.5091	1.5083	1.5076	49.59	521496
1.5002	1.4994	1.4988	1.4983	51.36	511514
1.5998	1.5985	1.5975	1.5963	24.57	623246

show comparable refractive indices n_d (between 1.51 and 1.52) and dispersions represented by the Abbe numbers between 47 and 51. IP-Dip, in contrast, has a higher refractive index n_d above 1.55 and stronger dispersion represented by an Abbe number of 36 and PO4 has the highest refractive index n_d above 1.62 and an Abbe number of 25, thus the strongest dispersion. In comparison to the values that were obtained with 5 minutes UV exposure from [21] the refractive indices and Abbe numbers rise for all photoresists due to the stronger polymerization except for OrmoComp, which is more UV sensitive and therefore already almost entirely polymerized after 5 minutes of UV exposure.

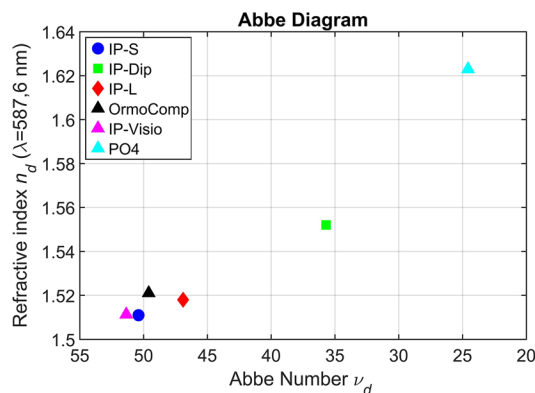


Fig. 7. Abbe diagram of the almost entirely polymerized photoresists. IP-S, IP-L, OrmoComp, and IP-Visio all have similar refractive indices n_d between about 1.51 and 1.52 with high Abbe numbers between 47 and 51. IP-Dip has a higher refractive index n_d above 1.55 and an Abbe number of 36 and PO4 has the highest refractive index n_d above 1.62 and an Abbe number of 25 indicating much stronger dispersion.

This result is helpful for the choice of photoresists for achromatic optical devices and elements, as different Abbe numbers are required. To realize achromatic functionality one should combine IP-Dip or PO4, which are outstanding for a high dispersion and refractive index, with one of the other photoresists, for example IP-S [1].

3.6. Extinction measurements

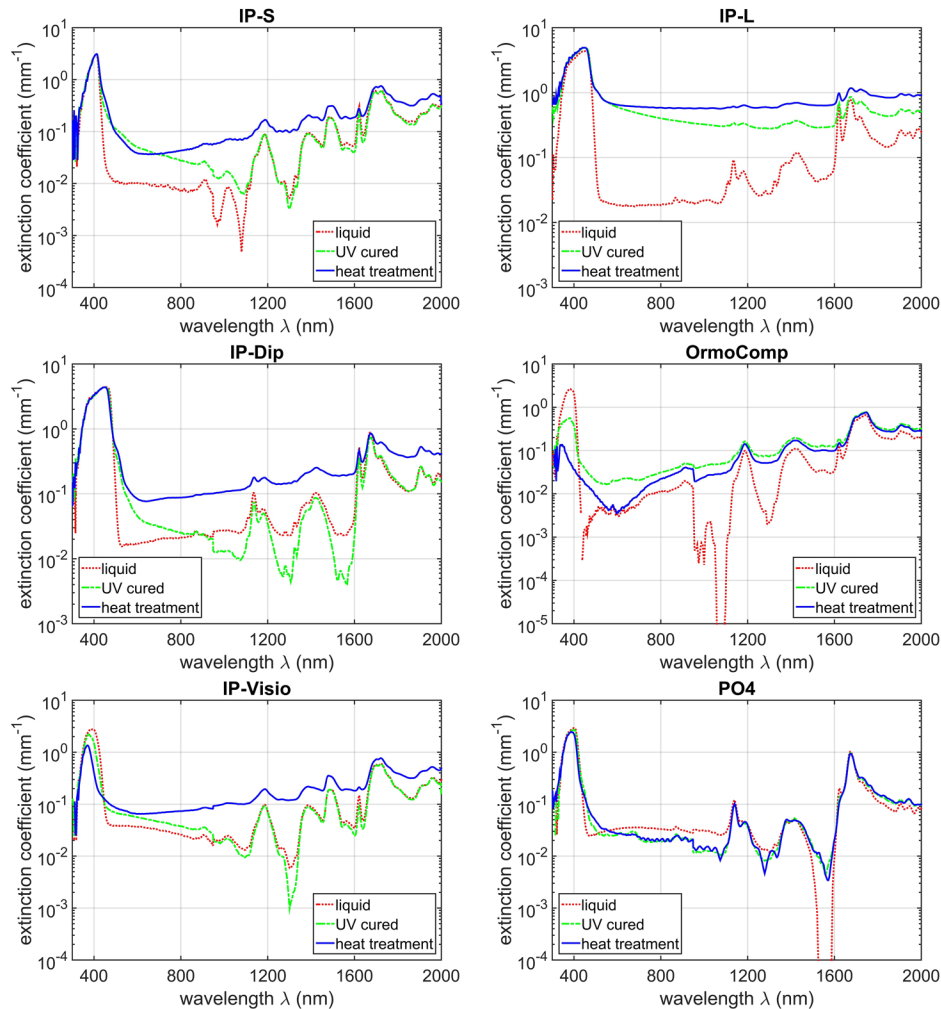


Fig. 8. Extinction of the photoresists IP-S, IP-Dip, IP-L, OrmoComp, IP-Visio, and PO4 in the liquid, UV treated and almost entirely polymerized state after heat treatment. The samples have been UV cured for 15 minutes and afterwards post baked at 60 °C for 1 hour.

In addition to the refractive indices we also measured the extinction coefficients (extinction = $-\ln[\text{transmission}]$) for 1 mm thick samples where the photoresist was embedded between two microscope slides and 1-photon UV hardened for 15 minutes. The measurements were referenced to two 1 mm microscope slides with a thin film (micrometer thickness) of the investigated photoresist to account for Fresnel reflection on the surface. We measured the different photoresists with a UV-VIS spectrometer (Zeiss detector NIR - MCS611 2.2 and VIS - MCS621 visII, light source CLH600) from 300 nm to 2000 nm in the liquid state, after 15 minutes

UV curing (OrmoComp just 1.5 minutes) and after additional heat treatment (1 hour at 60 °C), see Fig. 8. Due to the detector change at 950 nm a discontinuity in the absolute extinction value occurs. The error in the extinction coefficient is around 10-15%.

For all photoresists, the extinction has a local maximum at around 400 nm due to the photo initiator. The extinction values decrease to a local minimum at around 600 nm and increase for higher wavelengths, due to molecular vibration overtones.

The extinction behavior of IP-S, IP-Dip, and IP-Visio is very similar, whereas IP-L exhibits the highest extinction which shows very little variations over the spectral range. OrmoComp and PO4 exhibit the lowest extinction values followed by IP-S, which can be observed in Fig. 9. That makes them the appropriate choice for applications with thicker optical elements. Additional vibrational overtones are visible in the near-IR range.

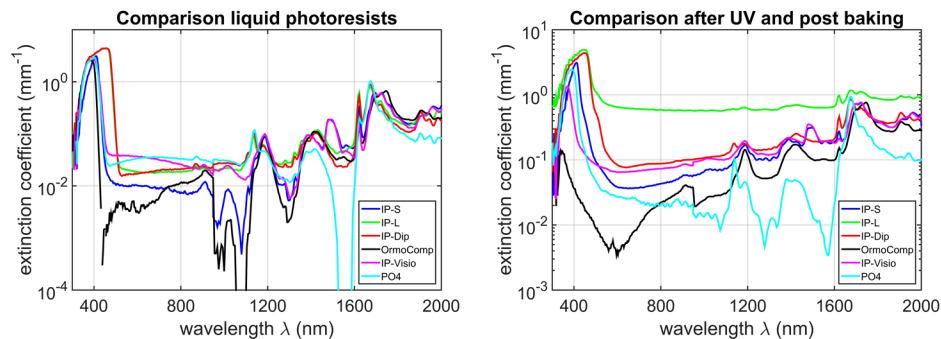


Fig. 9. Extinction of the photoresists IP-S, IP-Dip, IP-L, OrmoComp, IP-Visio, and PO4 in the liquid state and after UV curing and heat treatment. The samples have been UV cured for 15 minutes and afterwards post baked at 60 °C for 1 hour. The extinction consistently increases from the liquid to the polymerized state for all photoresists.

3.7. Luminescence measurements

The final material property discussed in this paper is the photoresist luminescence, as it is an important property to know in the context of possible 3D-written security features [2] as well as for possible use in 3D printed fluorescence microscope optics. We measure the luminescence with a Nikon Eclipse LV100 upright microscope using a Princeton Instruments Isoplan 160 with a Pixis 256e CCD camera. For excitation we use a Nikon super high pressure mercury lamp. We performed the measurements for all photoresists in the liquid state, after 15 minutes of UV curing and after additional heat treatment. The results are displayed in Fig. 10. The excitation wavelength is 390 +/- 18 nm with an exposure time of 15 seconds with 10 accumulations. All photoluminescence spectra are recorded with the same excitation conditions and recording times to allow for *quantitative* photoluminescence comparisons.

All photoresists show a strong luminescence maximum around 500 nm. The UV curing and heat treatment decrease the maximum at 500 nm for IP-L and IP-Dip, while it is shifted to slightly higher wavelengths for IP-S and IP-Visio. IP-S shows a factor 6 smaller luminescence in the liquid state than IP-Dip and IP-L which reduces to a factor 2-3 after UV curing and heat treatment. OrmoComp, IP-Visio, and PO4 exhibit more than an order of magnitude lower luminescence, which increases with UV curing and heat treatment. This makes them the appropriate choice for applications where low background luminescence in the visible is required. The different luminescence intensities are compared in Fig. 11.

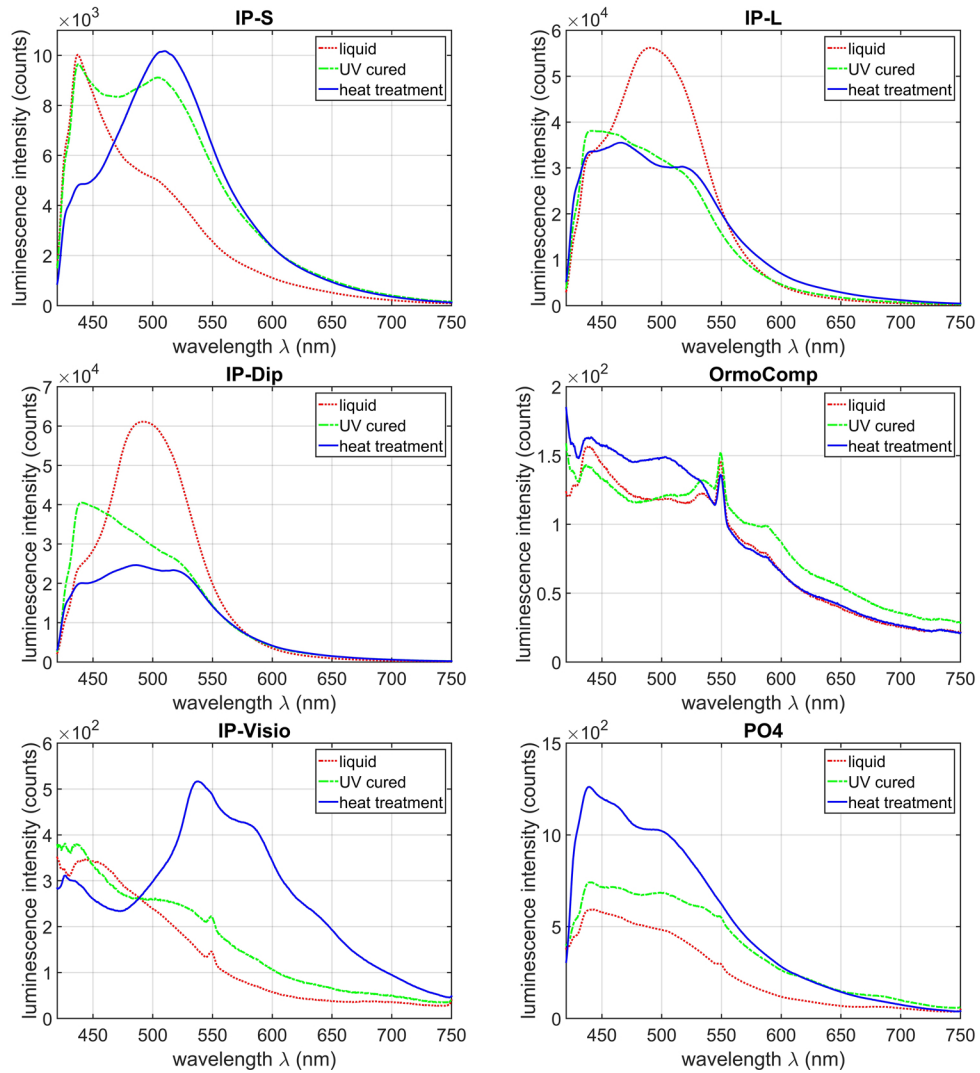


Fig. 10. Luminescence of the photoresists IP-S, IP-Dip, IP-L, OrmoComp, IP-Visio, and PO4 in the liquid, UV treated and almost entirely polymerized state after heat treatment. The samples have been UV cured for 15 minutes and afterwards post baked at 60 °C for 1 hour.

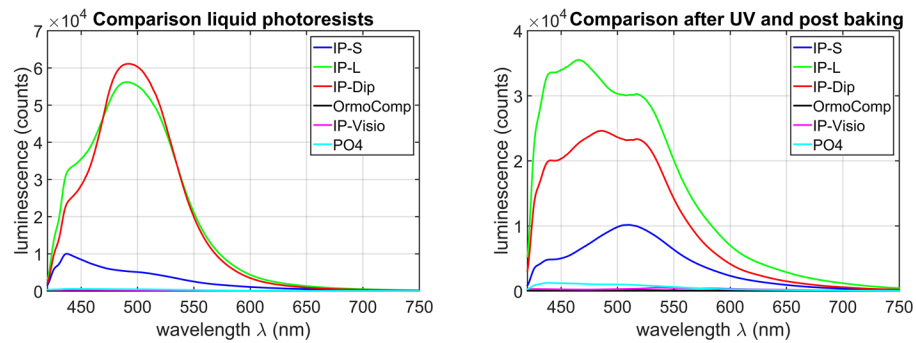


Fig. 11. Luminescence of the photoresists IP-S, IP-Dip, IP-L, OrmoComp, IP-Visio, and PO4 after UV curing and heat treatment upon comparable excitation and data acquisition conditions. The samples have been UV cured for 15 minutes and afterwards post baked at 60 °C for 1 hour. OrmoComp shows by far the lowest luminescence, followed by IP-Visio, PO4 and IP-S. IP-L and IP-Dip show very similar results with the highest luminescence among the photoresists at around 500 nm.

4. Conclusion

In this work we measured the refractive index dispersion in the visible and near IR spectral range for six different photoresists, namely IP-S, IP-Dip, IP-L, OrmoComp, IP-Visio, and PO4.

We studied the different effects of UV dose, aging, heat treatment, and 2-photon writing on the refractive indices of IP-S, IP-Dip, IP-L, and OrmoComp. For all photoresists the refractive index increases and saturates with the UV duration and the aging process. Using heat treatment for 1 hour at 60 °C is sufficient to increase the polymerization process to achieve almost entire polymerization even with short UV exposure durations. Due to the used high laser power, our 2-photon polymerized structures are also almost entirely polymerized, sufficient small hatching and slicing provided (which was not achieved for IP-Dip). Using lower intensities, the refractive index of 2-photon polymerized photoresists can also change [20]. We performed wide range measurements from 405 nm to 1400 nm for the almost entirely polymerized photoresists and also provide the Abbe numbers to compare the dispersions as well as Sellmeier fits that give best agreement between model and experiments.

The extinction of the photoresists is also increased during the polymerization process. The luminescence spectra of all photoresists show a maximal luminescence around 500 nm, OrmoComp, IP-Visio, and PO4 show the smallest luminescence.

Funding

Deutsche Forschungsgemeinschaft (GI 269/12-1); Bundesministerium für Bildung und Forschung (13N14097, PRINTFUNCTION, PRINTOPTICS); Baden-Württemberg Stiftung (OPTERIAL, Spitzenforschung II); H2020 European Research Council (COMPLEXPLAS); European Research Council (PoC 3D PRINTEDOPTICS).

Acknowledgments

We thank David Neußer and Sabine Ludwigs for help with their UV-VIS spectrometer. We also thank Simon Thiele for advice with Zemax OpticStudio. This publication was supported by the Open Access Publishing Fund of the University of Stuttgart.

References

1. M. Schmid, S. Thiele, A. Herkommer, and H. Giessen, "Three-dimensional direct laser written achromatic axicons and multi-component microlenses," *Opt. Lett.* **43**(23), 5837 (2018).
2. F. Mayer, S. Richter, P. Hübner, T. Jabbour, and M. Wegener, "3D Fluorescence-Based Security Features by 3D Laser Lithography," *Adv. Mater. Technol.* **2**(11), 1700212 (2017).
3. M. Deubel, M. Wegener, S. Linden, G. von Freymann, and S. John, "3D-2D-3D photonic crystal heterostructures fabricated by direct laser writing," *Opt. Lett.* **31**(6), 805 (2006).
4. C. Liberale, G. Cojoc, P. Candeloro, G. Das, F. Gentile, F. De Angelis, and E. Di Fabrizio, "Micro-Optics Fabrication on Top of Optical Fibers Using Two-Photon Lithography," *IEEE Photonics Technol. Lett.* **22**(7), 474–476 (2010).
5. M. Kowalczyk, J. Haberko, and P. Wasylczyk, "Microstructured gradient-index antireflective coating fabricated on a fiber tip with direct laser writing," *Opt. Express* **22**(10), 12545 (2014).
6. N. Lindenmann, G. Balthasar, D. Hillerkuss, R. Schmogrow, M. Jordan, J. Leuthold, W. Freude, and C. Koos, "Photonic wire bonding: a novel concept for chip-scale interconnects," *Opt. Express* **20**(16), 17667 (2012).
7. T. Gissibl, S. Thiele, A. Herkommer, and H. Giessen, "Sub-micrometre accurate free-form optics by three-dimensional printing on single-mode fibres," *Nat. Commun.* **7**(1), 11763 (2016).
8. G. von Freymann, A. Ledermann, M. Thiel, I. Staude, S. Essig, K. Busch, and M. Wegener, "Three-Dimensional Nanostructures for Photonics," *Adv. Funct. Mater.* **20**(7), 1038–1052 (2010).
9. T. Gissibl, S. Thiele, A. Herkommer, and H. Giessen, "Two-photon direct laser writing of ultracompact multi-lens objectives," *Nat. Photonics* **10**(8), 554–560 (2016).
10. S. Thiele, T. Gissibl, H. Giessen, and A. M. Herkommer, "Ultra-compact on-chip LED collimation optics by 3D femtosecond direct laser writing," *Opt. Lett.* **41**(13), 3029 (2016).
11. T. Gissibl, M. Schmid, and H. Giessen, "Spatial beam intensity shaping using phase masks on single-mode optical fibers fabricated by femtosecond direct laser writing," *Optica* **3**(4), 448 (2016).
12. S. Thiele, K. Arzenbacher, T. Gissibl, H. Giessen, and A. M. Herkommer, "3D-printed eagle eye: Compound microlens system for foveated imaging," *Sci. Adv.* **3**(2), e1602655 (2017).
13. S. Wong, M. Deubel, F. Pérez-Willard, S. John, G. A. Ozin, M. Wegener, and G. von Freymann, "Direct Laser Writing of Three-Dimensional Photonic Crystals with a Complete Photonic Bandgap in Chalcogenide Glasses," *Adv. Mater.* **18**(3), 265–269 (2006).
14. M. Deubel, G. von Freymann, M. Wegener, S. Pereira, K. Busch, and C. M. Soukoulis, "Direct laser writing of three-dimensional photonic-crystal templates for telecommunications," *Nat. Mater.* **3**(7), 444–447 (2004).
15. M. Malinauskas, A. Žukauskas, V. Purlys, K. Belazaras, A. Momot, D. Paipulas, R. Gadonas, A. Piskarskas, H. Gilbergs, A. Gaidukevičiūtė, I. Sakellari, M. Farsari, and S. Juodkasis, "Femtosecond laser polymerization of hybrid/integrated micro-optical elements and their characterization," *J. Opt.* **12**(12), 124010 (2010).
16. J.-J. Xu, W.-G. Yao, Z.-N. Tian, L. Wang, K.-M. Guan, Y. Xu, Q.-D. Chen, J.-A. Duan, and H.-B. Sun, "High Curvature Concave–Convex Microlens," *IEEE Photonics Technol. Lett.* **27**(23), 2465–2468 (2015).
17. D. Wu, S.-Z. Wu, L.-G. Niu, Q.-D. Chen, R. Wang, J.-F. Song, H.-H. Fang, and H.-B. Sun, "High numerical aperture microlens arrays of close packing," *Appl. Phys. Lett.* **97**(3), 031109 (2010).
18. P.-I. Dietrich, M. Blaicher, I. Reuter, M. Billah, T. Hoose, A. Hofmann, C. Caer, R. Dangel, B. Offrein, U. Troppenz, M. Moehrl, W. Freude, and C. Koos, "In situ 3D nanoprinting of free-form coupling elements for hybrid photonic integration," *Nat. Photonics* **12**(4), 241–247 (2018).
19. R. Guo, S. Xiao, X. Zhai, J. Li, A. Xia, and W. Huang, "Micro lens fabrication by means of femtosecond two photon photopolymerization," *Opt. Express* **14**(2), 810 (2006).
20. S. Dottermusch, D. Busko, M. Langenhorst, U. W. Paetzold, and B. S. Richards, "Exposure-dependent refractive index of Nanoscribe IP-Dip photoresist layers," *Opt. Lett.* **44**(1), 29 (2019).
21. T. Gissibl, S. Wagner, J. Sykora, M. Schmid, and H. Giessen, "Refractive index measurements of photo-resists for three-dimensional direct laser writing," *Opt. Mater. Express* **7**(7), 2293 (2017).
22. J. Rys, S. Steenhusen, C. Schumacher, C. Cronauer, and C. Daraio, "Locally addressable material properties in 3D micro-architectures," *Extrem. Mech. Lett.* **28**, 31–36 (2019).